CLIMATOLOGY

Amplified warming of droughts in southern United States in observations and model simulations

Felicia Chiang[1]*, Omid Mazdiyasni[1], Amir AghaKouchak[1,2]

During droughts, low surface moisture may translate surface heating into warming, since excess energy will be converted into sensible heat instead of evaporating as latent heat. Recent concurrent occurrences of droughts and heatwaves have caused compounding ecosystem and societal stresses, which prompted our investigation of whether there has been a shift in temperatures under meteorological drought conditions in the United States. Using historical observations, we detect that droughts have been warming faster than the average climate in the southern and northeastern United States. Climate model projections also show a pronounced warming shift in southern states between the late 20th and 21st centuries. We argue that concurrent changes in vapor pressure deficit and relative humidity influence the amplified warming, modifying interactions between the land surface and the atmosphere. We anticipate that the magnified shift in temperatures will bring more concurrent extremes in the future, exacerbating individual impacts from high temperatures and droughts.

INTRODUCTION

The concurrence of drought and heatwave events has caused severe ecosystem and societal stresses, as witnessed during 2014 in California and 2003 in Europe (*1*, *2*). Land surface and atmosphere interactions have been identified as a major driver in the occurrence of these concurrent extremes. During dry soil moisture conditions, we expect to see associated surface warming, as the available energy will be expressed as sensible heat instead of being evaporated as latent heat, causing the concurrence of these conditions (*3–5*). For example, in the European heatwave event, precipitation deficits in the Mediterranean region were noted to precede major heatwaves in neighboring regions (*6*).

These short-term temperature changes are dependent on the negative and positive feedbacks between the local land surface condition and the atmosphere above (*7–11*). In addition to temperature changes, low soil moisture in mid-continental areas can alter planetary boundary layer dynamics that influence precipitation (*12*). In contrast, coastal areas experience a thermal difference between the land and the sea, which is magnified during periods of dry soil, resulting in an increased transport of moist air from the oceans (*12*). Through many studies, land surface and atmosphere interactions have been established as major climate drivers (*3–5*). However, the feedbacks and interactions between components of the land surface and the atmosphere have not been fully understood and quantified. Moreover, we still do not completely understand the full spectrum of changes that will accompany the simple increase in greenhouse gases, such as compounding extreme events (*13*).

Here, we examine long-term shifts in temperatures occurring during dry months to further explore feedbacks between surface moisture and temperature conditions (fig. S1). Drawing from established interactions between drying and warming conditions, we study whether temperatures during droughts have experienced changes in the 20th century and whether shifts in dry temperatures will occur under projected climate change conditions. We also evaluate changes in uncertainty that have occurred under observed and projected meteorological drought conditions in comparison to average climate conditions. Because of projections showing droughts and high temperatures intensifying over the next century, the goal of the study is to understand whether tempera-

tures are projected to experience different rates of intensification when coupled with dry conditions. We hope to evaluate whether conditional temperature shifts under droughts are occurring while acknowledging the possible drivers of land surface–atmosphere interactions and feedbacks under climate change. We also examine changes in atmospheric moisture to evaluate concurrent shifts in the climate system.

For this study, we evaluate temperatures during different drought severities in two observed periods (1902–1951 and 1965–2014) and two modeled periods (1951–2000 and 2050–2099) in the contiguous United States. For the observations, we compare the late 20th century to the early 20th century to quantify temperature changes that have already occurred. For the model ensemble, we compare the late 21st and late 20th century periods to investigate future conditions relative to the recent historical past. We defined drought severities on the basis of the U.S. Drought Monitor: with the D_0 threshold equivalent to a standardized precipitation index (SPI) of −0.5 or lower and the D_1 threshold equivalent to an SPI of −0.8 or lower (see Materials and Methods for further explanation). To evaluate coincident changes under atmospheric moisture conditions, we used relative humidity and vapor pressure deficit (VPD) as quantitative measures of available moisture.

RESULTS

Between the early and late 20th century observations from the Climatic Research Unit (CRU), the southern and northeastern United States experienced greater temperature shifts under dry conditions than the average climate (Fig. 1A). The southern states experienced a similar pattern of change in the downscaled Coupled Model Intercomparison Project Phase 5 (CMIP5) multimodel ensemble (Fig. 1B). In the observations, the regions associated with amplified temperature change under the D_0 and D_1 thresholds contrasted with the warming regions highlighted in the average temperature change panel, indicating that the observed pattern was not temperature-driven. The accelerated warming under dry conditions also does not correspond with regions commonly identified as semiarid or arid. For example, the southern United States experiences a dry climate in the west and a humid climate in the east; however, all southern states experience similar accelerations in warming under dry conditions.

Around the globe, increasing aridity has been attributed to more rapid increases in evaporative demand relative to precipitation supply

[1]Department of Civil and Environmental Engineering, University of California, Irvine, CA 92697–2175, USA. [2]Department of Earth System Science, University of California, Irvine, CA 92697–3100, USA.
*Corresponding author. Email: chiangf@uci.edu

(14–16). This increase in aridity has been expressed in decreasing relative humidity and increasing VPD shown in Fig. 2 (A and B) (15–17). Under the D_0 and D_1 thresholds, we observe concurrent increases and decreases in temperature, relative humidity, and VPD across the United States (Figs. 1A and 2, A and B). In regions where temperature shifts under droughts have outpaced temperature changes in the average climate, relative humidity has decreased and VPD has increased. For example, in the northeastern region in Figs. 1A and 2 (A and B), we see positive temperature shifts corresponding with decreases in relative humidity and increases in VPD.

We also observe corresponding increases in moisture in regions where temperature shifts under the average climate have outpaced shifts under drought. For instance, in the upper Midwestern region, we see negative temperature shifts relating to increases in relative humidity and decreases in VPD (Figs. 1A and 2, A and B). McHugh *et al.* (18) recently established that nonrainfall water sources—such as atmospheric moisture—can act as a significant source of moisture in drylands during periods when the relative humidity in the soil is lower than that of the air above. This finding explains the mechanism behind stagnant or cooling temperature shifts under drought conditions with respect to average

temperatures. The effect of water vapor on soil moisture (and by proxy, land surface warming) highlights the importance of the general dryness or wetness of the area, which cannot be attributed to a single variable. In all regions, we hypothesize that, during periods of drought, the concurrent shift in atmospheric moisture contributes to the amplification of temperature changes relative to the average climate. Note that, when considering all months, wet or dry, this concurrence does not occur between the variables (see first column in Figs. 1A and 2, A and B). This highlights the importance of meteorological drought in strengthening the correlation between changes in atmospheric moisture and temperature (19).

We argue that the decreasing availability of regional moisture relative to evaporative demand may be the driving force shaping the spatial pattern of temperature, relative humidity, and VPD changes. Changes in relative humidity and VPD are the physical manifestations of the limits on land evaporation (16). The limit on land evaporation will increase the amount of local sensible heat, subsequently leading to a relative warming of the land surface. As we observe in our results, this is amplified during periods of drought. Although observed increases in temperature have increased the upper limit of saturation vapor pressure, the relative lack
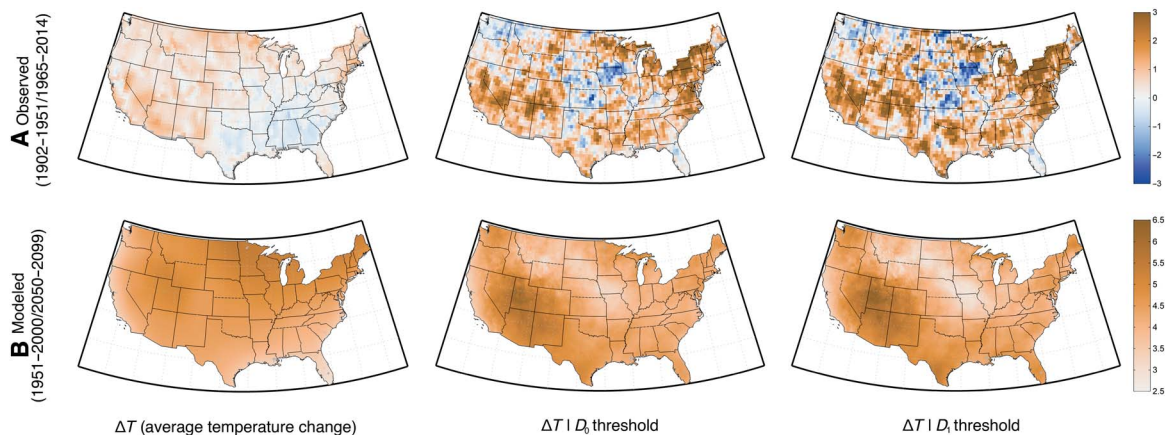
Fig. 1. Temperature shift associated with each dryness condition. Average temperature shift relating to each condition (including all wet and dry conditions, at or under the D_0 threshold, and at or under the D_1 threshold). (**A**) We compare the period of 1965–2014 relative to a baseline period of 1902–1951 with the observed CRU data. (**B**) We compare the future period of 2050–2099 relative to the historical baseline period of 1951–2000 with the CMIP5 model average ensemble.
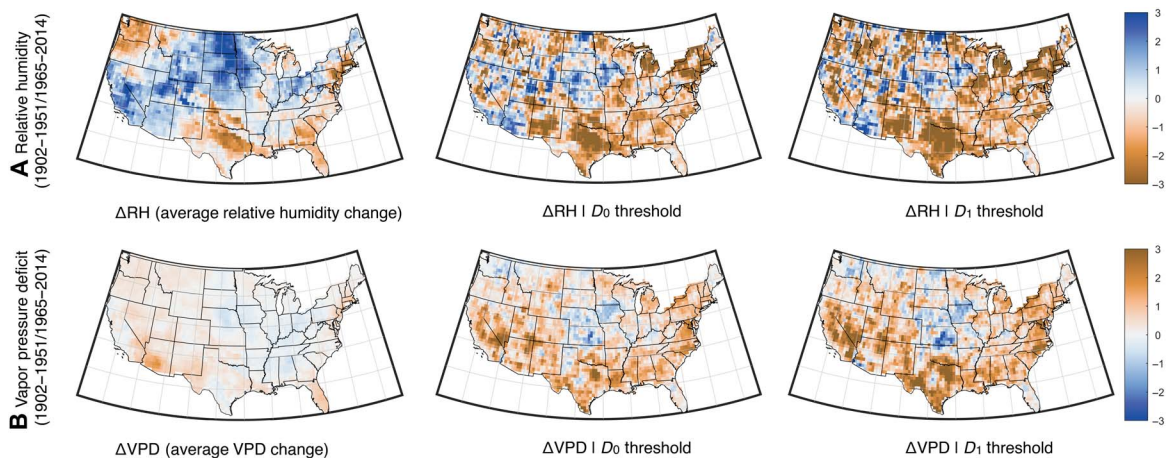

Fig. 2. Moisture shift associated with each dryness condition. Average shift between the period 1965–2014 relative to the baseline period of 1902–1951 associated with each dryness condition used in Fig. 1. (**A**) Observed average shift in relative humidity associated with each condition. (**B**) Observed average shift in VPD associated with each condition.

of available moisture, especially during droughts, limits actual vapor pressure (16, 17).

We hypothesize that increases in drought frequencies due to the behavior of the Pacific Decadal Oscillation and the Southern Oscillation Index may have shaped the southern and eastern patterns in the observed shift (20). Changes in atmospheric circulation patterns and vertical transport of moisture due to climate change may have contributed to the spatial patterns in the shift (21). In addition, regional man-made changes in land cover may have resulted in changes in soil moisture and temperature (22). Dampened summer temperature highs have been associated with intensifying irrigation in the upper Midwestern region (23). These agriculturally influenced climate trends relate directly to the Midwestern cooling signal shown in Fig. 1A. In contrast, since the 1960s, annual snow cover extent has shrunken by 10% (24). The occurrence of snow cover significantly influences local temperatures due to albedo and emissivity properties of snow (25). Snowmelt also acts as a latent heat sink, increasing soil moisture levels and regulating local temperatures (25). Thus, a decrease in snow cover extent could be associated with an increase in surface temperature, corresponding with the amplified temperature shifts along the East Coast in Fig. 1A.

As shown in Fig. 1B, the spatial pattern of temperature change does not coincide with the north-to-south gradient of latitudinal heating predicted under the representative concentration pathway (RCP) 8.5 scenario. Instead of the north experiencing greater shifts in comparison to the south, our results display the opposite pattern. The spatial patterns where amplified shifts in temperature are projected to occur can also be seen in the patterns in relative humidity and VPD. CMIP5 ensembles have predicted changes in water vapor concentrations and changes throughout the hydrologic cycle due to projected climate change, causing shifts in the distributions of precipitation and evaporation around the globe (26). Significant decreases in the difference between precipitation and surface evaporation are projected to occur in the southern regions across all seasons (27), corresponding to the temperature conditions displayed in Fig. 1B.

Regional delineations in Figs. 3 and 4 highlight the differences between the historical observations and model projections. Historically, the northeastern region of the United States shows the amplified drought-associated temperature shift, while CMIP5 models predict a smaller, more muted future shift in temperature with respect to the average climate in the entire upper half of the United States, including the northeast. CRU observations show that the median dry temperature shifts 0.81° higher than the average climate when we isolate regions with amplified temperature shifts. In the CMIP5 projections, the median dry temperature shifts 0.30° higher than the average climate in the regions with amplified temperature change. The shifts quantified in the observations and models show the influence of dry periods on the increasing intensity of climate conditions in the southern United States. These changes occurred for VPD and relative humidity as well.

We also note that the range of temperature uncertainty is dependent on the climate condition. In the CRU observations, temperature shifts in the average climate condition exhibit minimal variability in comparison to the shifts under the D_0 and D_1 threshold conditions (Fig. 3). In addition, the more severe D_1 condition exhibits larger ranges of temperature variability relative to the milder D_0 condition, as seen in all regions in the United States. This implies that drier temperature conditions generally experience larger ranges of uncertainty over each region.

We also plotted cumulative distribution functions of the temperature shifts under different dryness conditions to illustrate distributional changes between the periods. Figure 5A shows that observed temperatures in the southeastern United States shift to the right under D_0 drought conditions. A shift to the right represents more severe temperature conditions. Figure 5B also shows the modeled temperature distribution under the D_0 condition, increasing the emphasis on warmer months in comparison to the average climate. Distributional plots for the remaining regions reflect the results from the boxplot figures (figs. S2 and S3).

The Kolmogorov-Smirnov (K-S) and Student's t tests revealed statistically significant differences between the shifts seen from average
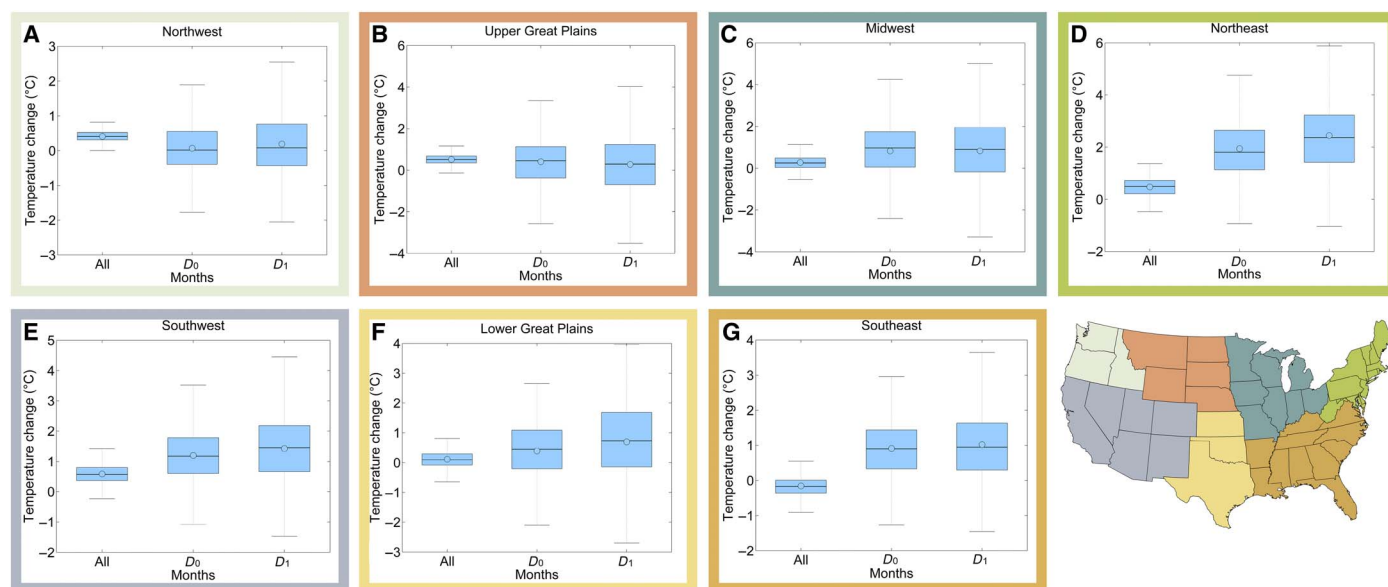

Fig. 3. Regional boxplots for observations. (**A** to **G**) Regional boxplots displaying the temperature shifts corresponding to each dryness condition for the CRU observations (1965–2014 relative to 1902–1951).
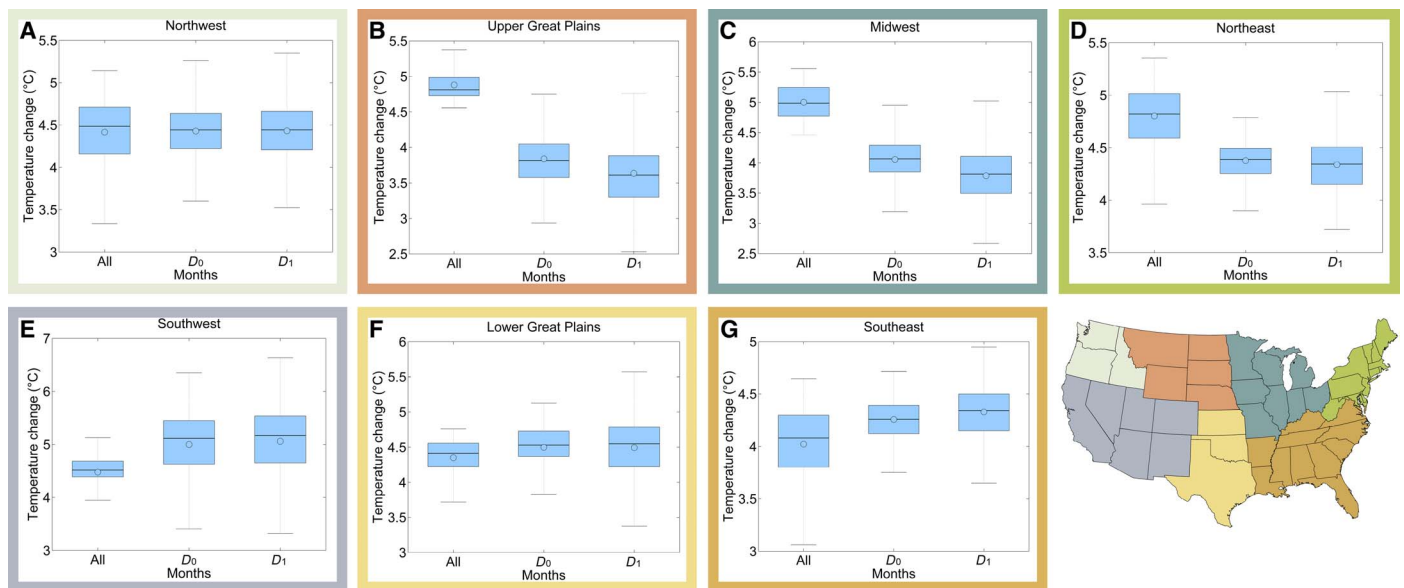
Fig. 4. Regional boxplots for model ensemble. (**A** to **G**) Regional boxplots displaying the temperature shifts corresponding to each dryness condition for the CMIP5 model ensemble (2050–2099 relative to 1951–2000).
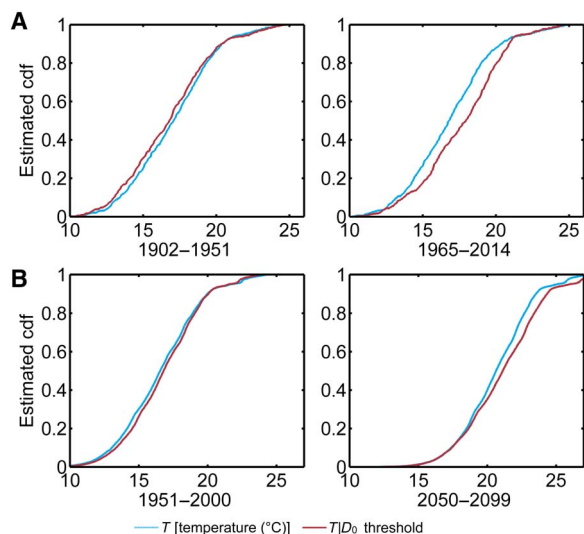

Fig. 5. Distributional shift associated with southeastern United States. Distributional plots comparing the shifts between the D_0 condition and the average climate for the southeastern region of the United States. (**A**) We compare the period of 1965–2014 relative to a baseline period of 1902–1951 with the observed CRU data. cdf, cumulative distribution function. (**B**) We compare the future period of 2050–2099 relative to the historical baseline of 1951–2000 with the CMIP5 model average ensemble.

temperatures and those seen under the D_0 threshold in the two observational periods in all regions. The K-S test also showed statistically significant differences between the average temperature and D_0 threshold shifts in comparing the future projections relative to the modeled past. T testing showed that all regions, except the northwest, show statistically significant differences between the dry and average temperature shifts. The statistical tests highlight that all amplified temperature shifts occurring under drought conditions in the observations and models are significantly different from temperature shifts occurring under average climate conditions.

DISCUSSION

The observed and projected amplifications in temperature change in the southern United States will have severe ramifications in environmental and social sectors. Droughts alone have had severe urban, agricultural, and ecological impacts in recent years, directly and indirectly reducing water availability (28). Warm periods have also affected many of the same sectors by stressing vulnerable populations, food resources, energy, and transportation systems (28, 29). We expect the concurrence of droughts and warm events to physically manifest in more frequent wildfires, reduced air quality, and stressed agricultural crops and livestock (29).

Under our future projections of amplified drought-conditioned temperature shifts in the southern United States, the occurrence of concurrent extremes will likely increase and exacerbate the impacts anticipated from individual extremes. This is exceedingly important as dry lands are becoming more widespread under climate change, which will widen the documented temperature impact (30, 31). In addition, these conditional temperature shifts will compound on the increased probability of more extreme, warm events in projected pathways of climate warming (32). We anticipate severe socioeconomic consequences to accompany these drought-conditioned temperature shifts. The consequences may include disruptions of local and global food systems, damages to public health and quality of life, and the expansion of areas vulnerable to concurrent extremes (33). Society can respond to these observed and projected concurrent events by studying the effects of these natural threats and improving the resilience of our systems to these threats. Future studies should focus on the ramifications of these temperature shifts to quantify projected risks on population health, food supply, and infrastructure. From these studies, we can propose changes in urban development and settlement patterns to reduce population exposure to extremes, improve agricultural cultivation and trade, and adapt building infrastructure to the changing climate—all responses that can alleviate the negative impacts of these intensifying extremes (33).

The accuracy of our observations and model projections limits our interpretations of the findings. In some areas, the CMIP5 models may have inconsistent physical interpretations since representations of land

surface and atmospheric interactions vary across models. Although the models capture large-scale temperature patterns, extreme precipitation events are still not adequately represented (21, 27). The capture of extreme precipitation events has the potential to affect the timing of dry and wet periods in the models. Projections of El Niño–Southern Oscillation timing and variability also suffer from model biases (21). The CMIP5 projections also have trouble with warm and cool sea surface temperature biases in the Pacific and Atlantic Oceans (21). Donat et al. (34) also highlights that high temperature extremes have been increasing faster than mean temperatures but show CMIP5 model inconsistencies with observations over much of the globe. The known errors in the CMIP5 output prevent us from drawing concrete conclusions from the differences between the observations and the projections.

Observations show that amplified temperature shifts have been occurring under drought conditions relative to temperature changes occurring under average climate conditions in the southern and northeastern regions of the United States. The spatial pattern of the drought-conditioned temperature shift can largely be associated with observed shifts in atmospheric moisture content such as relative humidity and VPD. Although we cannot define which variable is the driver at this temporal scale, both temperature and moisture shifts are interacting and amplifying under drought conditions. Projections show that droughts will be significantly warmer than average conditions across the southern region of the United States and are also associated with modeled shifts in relative humidity and VPD. This study highlights the importance of atmospheric moisture in the absence of precipitation in driving changes in the energy and hydrologic cycles.

MATERIALS AND METHODS
Experimental design
For our observations, we used monthly temperature, precipitation, and vapor pressure data available from the CRU TS3.23, which is a gridded time series climate dataset (35). The data coverage included all areas of the contiguous United States at a 0.5° resolution. Estimates for saturated vapor pressure (e_s) were derived using the 2008 World Meteorological Organization Commission for Instruments and Methods of Observation Guide conversion equation

$$e_s = 6.112 \times \exp\left(\frac{22.46t}{272.62 + t}\right) \tag{1}$$

where t is the temperature at a given grid point at a given time.

Relative humidity (RH) was derived with the standard equation from saturated and actual vapor pressure (e_a)

$$\text{RH} = \frac{e_a}{e_s} \times 100\% \tag{2}$$

For the model projections, we used the bias-corrected spatially disaggregated (BCSD) downscaled CMIP5 multimodel ensemble under RCP 8.5 at a 0.125° resolution available from the U.S. Bureau of Reclamation website (36). The BCSD method is a statistical downscaling method that uses the probability density functions of model output mapped onto observations and then spatially aggregates the results to the desired scale (37). We took an average of the models listed in the Supplementary Materials to form the model ensemble. The CMIP5 models are the most recent internationally coordinated collection of climate models used to estimate historical observations and project how the climate will change in the future (21). We chose to use the CMIP5 multimodel ensemble under RCP 8.5 to evaluate average projected future temperature conditions under a "business as usual" emission scenario.

We used the SPI as a measure of the relative meteorological dryness of each pixel in the spatial area of interest. For our study, we used a nonparametric implementation of the SPI to retain the spatial and temporal consistency of the original data while describing precipitation in the context of the local climatology (19). We used the empirical Gringorten plotting position

$$p(x_i) = \frac{i - 0.44}{n + 0.12} \tag{3}$$

where n is the sample size, i is the rank of nonzero precipitation data from smallest to largest, and $p(x_i)$ is the empirical probability for each data point (19). We standardized the probabilities, p, from Eq. 3 using the standard normal distribution function, ϕ (19)

$$\text{SI} = \phi^{-1}(p) \tag{4}$$

Although drought can be characterized by many timescales, we chose to use a 6-month timescale to capture intra-annual seasons without including overly brief wet or dry periods.

We first calculated the average temperature shift associated with each dryness threshold for each pixel. To find the temperature shift between periods, we calculated the difference between the temperature averages associated with the two periods. We used the U.S. Drought Monitor classification scheme (D_0, D_1, D_2, etc.) to define the drought severity thresholds. D_0 began with an SPI of −0.5, D_1 began with an SPI of −0.8, and D_2 began with an SPI of −1.3. For instance, for the D_0 threshold, we isolated months that had an SPI value of −0.5 or lower and found the corresponding temperature average. We then summarized the temperature shifts within seven climatically consistent regions in the contiguous United States. For average shifts of relative humidity and VPD between time periods, we used the same dryness thresholds for all pixels.

Statistical analysis
We used the two-sample K-S nonparametric test

$$D^* = \max_x \left(|\hat{F}_1(x) - \hat{F}_2(x)|\right) \tag{5}$$

where $\hat{F}_1(x)$ is the proportion of values in the first distribution less than or equal to x, and $\hat{F}_2(x)$ is the proportion of values in the second distribution less than or equal to x (38), and Student's two-sample t test

$$t = \frac{\bar{x} - \bar{y}}{\sqrt{\frac{s_x^2}{n} + \frac{s_y^2}{m}}} \tag{6}$$

where $\bar{x}$ and $\bar{y}$ are the sample means, s_x and s_y are the sample SDs, and n and m are the sample sizes for the two data samples (39), to determine whether regional shifts under the drier conditions were significant in comparison to the average temperature change experienced in the area ($\alpha = 0.05$). To conduct the statistical tests,

we used values from each pixel in each region from both average temperature conditions and dry temperature conditions. The two-sample K-S test determined whether data from average temperatures and data from dry temperature conditions originated from the same continuous distribution. The two-sample *t* test determined whether data from average temperatures and data from dry temperature conditions originated from populations with equal means or populations with statistically different means.

SUPPLEMENTARY MATERIALS

Supplementary material for this article is available at http://advances.sciencemag.org/cgi/content/full/4/8/eaat2380/DC1

Fig. S1. Flowchart describing the research methodology.
Fig. S2. Distributional shifts for observed United States.
Fig. S3. Distributional shifts for projected United States.
Table S1. CMIP5 climate models used.

REFERENCES AND NOTES

1. A. AghaKouchak, L. Cheng, O. Mazdiyasni, A. Farahmand, Global warming and changes in risk of concurrent climate extremes: Insights from the 2014 California drought. *Geophys. Res. Lett.* **41**, 8847–8852 (2014).
2. G. P. Asner, P. G. Brodrick, C. B. Anderson, N. Vaughn, D. E. Knapp, R. E. Martin, Progressive forest canopy water loss during the 2012–2015 California drought. *Proc. Natl. Acad. Sci. U.S.A.* **113**, E249–E255 (2016).
3. S. I. Seneviratne, D. Lüthi, M. Litchi, C. Schär, Land–atmosphere coupling and climate change in Europe. *Nature* **443**, 205–209 (2006).
4. E. M. Fischer, S. I. Seneviratne, D. Lüthi, C. Schär, Contribution of land-atmosphere coupling to recent European summer heat waves. *Geophys. Res. Lett.* **34**, L06707 (2007).
5. H. Su, Z.-L. Yang, R. E. Dickinson, J. Wei, Spring soil moisture-precipitation feedback in the Southern Great Plains: How is it related to large-scale atmospheric conditions? *Geophys. Res. Lett.* **41**, 1283–1289 (2014).
6. R. Vautard, P. Yiou, F. D'Andrea, N. de Noblet, N. Viovy, C. Cassou, J. Polcher, P. Ciais, M. Kageyama, Y. Fan, Summertime European heat and drought waves induced by wintertime Mediterranean rainfall deficit. *Geophys. Res. Lett.* **34**, L07711 (2007).
7. J. E. Walsh, W. H. Jasperson, B. Ross, Influences of snow cover and soil moisture on monthly air temperature. *Mon. Weather Rev.* **113**, 756–768 (1985).
8. F. Chang, J. M. Wallace, Meteorological conditions during heat waves and droughts in the United States Great Plains. *Mon. Weather Rev.* **115**, 1253–1269 (1987).
9. J. Huang, H. M. van den Dool, Monthly precipitation-temperature relations and temperature prediction over the United States. *J. Clim.* **6**, 1111–1132 (1993).
10. P. A. Dirmeyer, Y. Jin, B. Singh, X. Yan, Trends in land–atmosphere interactions from CMIP5 simulations. *J. Hydrometeorol.* **14**, 829–849 (2013).
11. B. Livneh, M. P. Hoerling, The physics of drought in the U.S. Central Great Plains. *J. Clim.* **29**, 6783–6804 (2016).
12. M. Stéfanon, P. Drobinski, F. D'Andrea, C. Lebeaupin-Brossier, S. Bastin, Soil moisture-temperature feedbacks at meso-scale during summer heat waves over Western Europe. *Clim. Dyn.* **42**, 1309–1324 (2014).
13. J. Zscheischler, S. Westra, B. J. J. M. van den Hurk, S. I. Seneviratne, P. J. Ward, A. Pitman, A. AghaKouchak, D. N. Bresch, M. Leonard, T. Wahl, X. Zhang, Future climate risk from compound events. *Nat. Clim. Chang.* **8**, 469–477 (2018).
14. J. T. Fasullo, Robust land–ocean contrasts in energy and water cycle feedbacks. *J. Clim.* **23**, 4677–4693 (2010).
15. A. Berg, K. Findell, B. Lintner, A. Giannini, S. I. Seneviratne, B. van den Hurk, R. Lorenz, A. Pitman, S. Hagemann, A. Meier, F. Cheruy, A. Ducharne, S. Malyshev, P. C. D. Milly, Land–atmosphere feedbacks amplify aridity increase over land under global warming. *Nat. Clim. Chang.* **6**, 869–874 (2016).
16. D. L. Ficklin, K. A. Novick, Historic and projected changes in vapor pressure deficit suggest a continental-scale drying of the U.S. atmosphere. *J. Geophys. Res. Atmos.* **122**, 2061–2079 (2017).
17. M. P. Byrne, P. A. O'Gorman, Understanding decreases in land relative humidity with global warming: Conceptual model and GCM simulations. *J. Clim.* **29**, 9045–9061 (2016).
18. T. A. McHugh, E. M. Morrissey, S. C. Reed, B. A. Hungate, E. Schwartz, Water from air: An overlooked source of moisture in arid and semiarid regions. *Sci. Rep.* **5**, 13767 (2015).
19. A. Farahmand, A. AghaKouchak, A generalized framework for deriving nonparametric standardized drought indicators. *Adv. Water Resour.* **76**, 140–145 (2015).
20. J. Kam, J. Sheffield, E. F. Wood, Changes in drought risk over the contiguous United States (1901-2012): The influence of the Pacific and Atlantic Oceans. *Geophys. Res. Lett.* **41**, 5897–5903 (2014).
21. Intergovernmental Panel on Climate Change, Climate change 2013: The physical science basis, in *Contribution of Working Group I to the Fifth Assessment Report of the Intergovernmental Panel on Climate Change*, T. F. Stocker, D. Qin, G.-K. Plattner, M. M. B. Tignor, S. K. Allen, J. Boschung, A. Nauels, Y. Xia, V. Bex, P. M. Midgley, Eds. (Cambridge Univ. Press, 2013).
22. H. Feng, Y. Liu, Combined effects of precipitation and air temperature on soil moisture in different land covers in a humid basin. *J. Hydrol.* **531**, 1129–1140 (2015).
23. N. D. Mueller, E. E. Butler, K. A. McKinnon, A. Rhines, M. Tingley, N. Michele Holbrook, P. Huybers, Cooling of US Midwest summer temperature extremes from cropland intensification. *Nat. Clim. Chang.* **6**, 317–322 (2016).
24. M. H. I. Dore, Climate change and changes in global precipitation patterns: What do we know? *Environ. Int.* **31**, 1167–1181 (2005).
25. T. Zhang, Influence of the seasonal snow cover on the ground thermal regime: An overview. *Rev. Geophys.* **43**, RG4002 (2005).
26. Z.-Q. Zhou, S.-P. Xie, X.-T. Zheng, Q. Liu, H. Wang, Q. Liu, H. Wang, Global warming–induced changes in El Niño teleconnections over the North Pacific and North America. *J. Clim.* **27**, 9050–9064 (2014).
27. J. Sheffield, A. Barrett, D. Barrie, S. J. Camargo, E. K. M. Chang, B. Colle, D. Nelun Fernando, R. Fu, K. L. Geil, Q. Hu, X. Jiang, N. Johnson, K. B. Karnauskas, S. Tae Kim, J. Kinter, S. Kumar, B. Langenbrunner, K. Lombardo, L. N. Long, E. Maloney, A. Mariotti, J. E. Meyerson, K. C. Mo, J. David Neelin, S. Nigam, Z. Pan, T. Ren, A. Ruiz-Barradas, R. Seager, Y. L. Serra, A. Seth, D.-Z. Sun, J. M. Thibeault, J. C. Stroeve, C. Wang, S.-P. Xie, Z. Yang, L. Yin, J.-Y. Yu, T. Zhang, M. Zhao, "Regional climate processes and projections for North American: CMIP3/CMIP5 difference, attribution and outstanding issues" (NOAA Technical Report OAR CPO-2, 2014).
28. C. Rosenzweig, W. D. Solecki, S. A. Hammer, S. Mehrota, *Climate Change and Cities: First Assessment Report of the Urban Climate Change Research Network* (Cambridge Univ. Press, 2011).
29. O. Mazdiyasni, A. AghaKouchak, Substantial increase in concurrent droughts and heatwaves in the United States. *Proc. Natl. Acad. Sci. U.S.A.* **112**, 11484–11489 (2015).
30. Q. Fu, S. Feng, Responses of terrestrial aridity to global warming. *J. Geophys. Res. Atmos.* **119**, 7863–7875 (2014).
31. L. Samaniego, S. Thober, R. Kumar, N. Wanders, O. Rakovec, M. Pan, M. Zink, J. Sheffield, E. F. Wood, A. Marx, Anthropogenic warming exacerbates European soil moisture droughts. *Nat. Clim. Chang.* **8**, 421–426 (2018).
32. V. V. Kharin, G. M. Flato, X. Zhang, N. P. Gillett, F. Zwiers, K. J. Anderson, Risks from climate extremes change differently from 1.5°C to 2.0°C depending on rarity. *Earth's Future* **6**, 704–715 (2018).
33. G. R. McGregor, M. Pelling, T. Wolf, S. N. Gosling, *The Social Impacts of Heatwaves* (Environmental Agency, 2003), 41 pp.
34. M. G. Donat, A. J. Pitman, S. I. Seneviratne, Regional warming of hot extremes accelerated by surface energy fluxes. *Geophys. Res. Lett.* **44**, 7011–7019 (2017).
35. I. Harris, P. D. Jones, T. J. Osborn, D. H. Lister, Updated high-resolution grids of monthly climatic observations—The CRU TS3.10 dataset. *Int. J. Climatol.* **34**, 623–642 (2014).
36. E. P. Maurer, L. Brekke, T. Pruitt, P. B. Duffy, Fine-resolution climate projections enhance regional climate change impact studies. *Eos. Trans. AGU* **88**, 504 (2007).
37. E. P. Maurer, H. G. Hidalgo, Utility of daily vs. monthly large-scale climate data: An intercomparison of two statistical downscaling methods. *Hydrol. Earth Syst. Sci.* **12**, 551–563 (2008).
38. F. J. Massey Jr., The Kolmogorov-Smirnov test for goodness of fit. *J. Am. Stat. Assoc.* **46**, 68–78 (1951).
39. J. H. McDonald, *Handbook of Biological Statistics* (Sparky House Publishing, 2008).

Citation: F. Chiang, O. Mazdiyasni, A. AghaKouchak, Amplified warming of droughts in southern United States in observations and model simulations. *Sci. Adv.* **4**, eaat2380 (2018).

Science Advances

Amplified warming of droughts in southern United States in observations and model simulations

Felicia Chiang, Omid Mazdiyasni and Amir AghaKouchak

ARTICLE TOOLS	http://advances.sciencemag.org/content/4/8/eaat2380
SUPPLEMENTARY MATERIALS	http://advances.sciencemag.org/content/suppl/2018/07/30/4.8.eaat2380.DC1
REFERENCES	This article cites 34 articles, 2 of which you can access for free http://advances.sciencemag.org/content/4/8/eaat2380#BIBL
PERMISSIONS	http://www.sciencemag.org/help/reprints-and-permissions

Use of this article is subject to the Terms of Service